



HAL
open science

Determination of the Intracellular Complexation of Inorganic and Methylmercury in Cyanobacterium *Synechocystis* sp. PCC 6803

Javier Garcia-Calleja, Thibaut Cossart, Zoyne Pedrero, João Santos, Laurent Ouerdane, Emmanuel Tessier, Vera Slaveykova, David Amouroux

► **To cite this version:**

Javier Garcia-Calleja, Thibaut Cossart, Zoyne Pedrero, João Santos, Laurent Ouerdane, et al.. Determination of the Intracellular Complexation of Inorganic and Methylmercury in Cyanobacterium *Synechocystis* sp. PCC 6803. *Environmental Science and Technology*, 2021, 55 (20), pp.13971-13979. 10.1021/acs.est.1c01732 . hal-03439343

HAL Id: hal-03439343

<https://hal.science/hal-03439343v1>

Submitted on 23 Nov 2021

HAL is a multi-disciplinary open access archive for the deposit and dissemination of scientific research documents, whether they are published or not. The documents may come from teaching and research institutions in France or abroad, or from public or private research centers.

L'archive ouverte pluridisciplinaire **HAL**, est destinée au dépôt et à la diffusion de documents scientifiques de niveau recherche, publiés ou non, émanant des établissements d'enseignement et de recherche français ou étrangers, des laboratoires publics ou privés.

1 **Determination of the intracellular complexation of inorganic and**
2 **methylmercury in cyanobacterium *Synechocystis* sp. PCC 6803.**

3
4 Javier Garcia-Calleja*¹, Thibaut Cossart², Zoyne Pedrero*¹, João P. Santos², Laurent Ouerdane¹,
5 Emmanuel Tessier¹, Vera I. Slaveykova², David Amouroux¹

6 ¹ Université de Pau et des Pays de l'Adour, E2S UPPA, CNRS, IPREM, Institut des Sciences
7 Analytiques et de Physico-chimie pour l'Environnement et les matériaux, Pau, France,

8 ² University of Geneva, Faculty of Sciences, Earth and Environment Sciences, Department F.-A.
9 Forel for Environmental and Aquatic Sciences, Uni Carl Vogt, 66 Bvd. Carl Vogt, CH-1211
10 Geneva, Switzerland

11
12 **Corresponding Authors:**

13 Javier Garcia-Calleja E-mail: javier.garcia-calleja@univ-pau.fr (J.C) phone: +34 669159412

14 Zoyne Pedrero E-mail: zoyne.pedrerorozayas@univ-pau.fr (Z.P) phone: +33 540175027

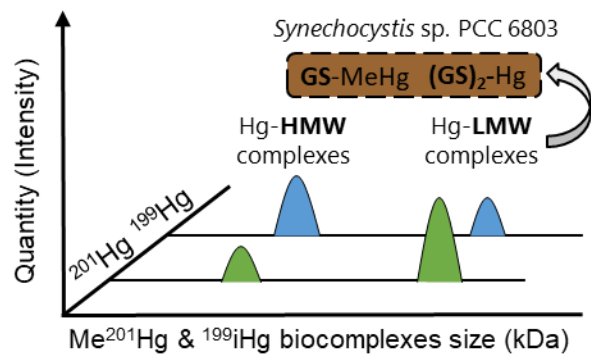
15

16 **ABSTRACT.**

17 Understanding of mercury (Hg) complexation with low molecular weight (LMW) bioligands will
18 help elucidate its speciation. In natural waters, the rate of this complexation is governed by
19 physicochemical, geochemical and biochemical parameters. However, the role of bioligands
20 involved in Hg intracellular handling by aquatic microorganisms is not well documented. Here,
21 we combine the use of isotopically-labelled Hg species (inorganic and monomethyl mercury, iHg
22 & MeHg) with gas or liquid chromatography coupling to elemental and molecular mass
23 spectrometry to explore the role of intracellular biogenic ligands involved in iHg and MeHg
24 speciation in cyanobacterium *Synechocystis* sp. PCC 6803, a representative phytoplankton species.
25 This approach allowed us to track resulting metabolic and newly-found intracellular Hg
26 biocomplexes (e.g. organic thiols) in *Synechocystis* sp. PCC 6803 finding different intracellular
27 Hg species binding affinities with both high and low molecular weight (HMW & LMW) bioligands
28 in the exponential and stationary phase. Furthermore, the parallel detection with both elemental
29 and molecular ionization sources allowed the sensitive detection and molecular identification of
30 glutathione (GSH) as the main low molecular weight binding ligand to iHg ((GS)₂-Hg) and MeHg
31 (GS-MeHg) in the cytosolic fraction. Such novel experimental approach expands our knowledge
32 on the role of biogenic ligands involved in iHg and MeHg intracellular handling in
33 cyanobacterium.

34 **KEYWORDS:** Phytoplankton, cyanobacteria, Hg speciation, LMW thiols, mass spectrometry,
35 glutathione.

36 **Graphical abstract:**



37

38

39 INTRODUCTION

40 Thiols are known to be important ligands for trace metals and known to affect the speciation of
41 several trace metals, such as Ag, Cd, Hg, their bioavailability and transformations in aquatic
42 environment. For example, thiols form complexes with inorganic mercury (iHg) and
43 monomethylmercury (MeHg) with structures of $\text{Hg}(\text{SR})_2$ or MeHgSR (R-S- being a thiolate
44 organic ligand)⁷. Therefore, the characterization of resulting Hg-biocomplexes together with their
45 quantification will provide an important information about the role of LMW thiol bioligands
46 involved in Hg speciation and bioavailability. Indeed, freshwater alga *Selenastrum capricornutum*
47 was exposed to MeHg complexed by environmental relevant thiols to study the influence of the
48 chemical structure and thermodynamic stability of MeHg complexes⁸. The complexation of iHg
49 and MeHg with bioligands, such as thiols, could also promote several abiotic and biotic
50 transformations such as reduction, methylation or demethylation but also, the iHg and MeHg
51 bioaccumulation¹⁰⁻¹². The intracellular bioligands could sequester Hg compounds thus
52 detoxifying mercury and affecting its trophic transfer^{13,14}. Beside our improved knowledge about
53 microbial Hg speciation in environment, the factors that control the intracellular iHg and MeHg
54 speciation and thus toxicity outcome are poorly understood.

55 Recent advanced state-of-the-art analytical methodologies for the determination of low molecular
56 weight (LMW) thiols in aquatic system have been developed based on a derivatization step with
57 several reagents to enhance their chemical stability before the analysis¹⁻⁵. Thiols can be separated
58 by liquid chromatography (LC) and detected by fluorescence¹, molecular absorption
59 (ultraviolet/visible detection)⁶ or electrospray ionization (ESI) coupled to tandem mass
60 spectrometry (LC-ESI-MS/MS)². For example, six LMW thiols (mercaptoacetic acid, cysteine,
61 homocysteine, N-acetyl-cysteine, mercaptoethane-sulfonate and glutathione) with concentrations

62 from 7 to 153 nM were determined in a freshwater lake and three boreal wetlands². Also, five
63 LMW thiols (cysteine, thioglycolic acid, N-acetyl-L-cysteine, 3-mercaptopropionic acid and
64 glutathione) were detected ranging from nM to μ M levels in wetland interstitial waters¹. Several
65 LMW thiols were found in benthic biofilm and green algae's periphyton dominated by cysteine
66 and 3-mercaptopropionic acid in the Bolivian Altiplano lakes³. Furthermore, studies focused on
67 biofilms revealed that the extracellular thiols concentration were up to 3 orders of magnitude
68 higher in biofilms than that in the surrounding water suggesting that microorganisms in the biofilm
69 could have a significant impact on Hg bioavailability through the excretion of LMW thiols⁵. The
70 quantification of 6 to 14 LMW thiol compounds with variable concentrations was also achieved
71 in the extracellular medium of anaerobic bacteria, in boreal wetland porewaters and in two coastal
72 sea waters⁴. Additionally, a recent novel analytical methodology was developed by optimizing
73 online preconcentration via solid phase extraction (SPE). Achieving detection limits at pM levels
74 and allowing the quantification of several MeHg-thiol complexes in the extracellular fraction of
75 the bacterium *Geobacter sulfurreducens* PCA previously exposed to 100 nM of iHg⁹. However,
76 the determination of Hg-biocomplexes in phytoplankton at environmental realistic concentration
77 has not been reported yet in aquatic system and need to be fulfilled for a better understanding of
78 the role of bioligands in Hg speciation.

79 Hyphenated techniques based on liquid chromatography coupled to inductively coupled plasma
80 mass spectrometry (ICP-MS) and/or molecular mass spectrometry have been implemented to look
81 into the wide spectrum at low and high molecular weight (HMW) Hg biocomplexes¹⁵. Particularly,
82 the use of hydrophilic interaction liquid chromatography (HILIC) coupled in parallel detection
83 with ICP-MS and ESI-MS/MS have been used to identify the structural characterization of several
84 metal-complexes in different biological matrices. For example, the identification of Hg bound to

85 several biothiols in plants¹⁶, the characterization of Hg-metallothioneins complexes in dolphin
86 liver¹⁷ and selenium metabolites in human urine and blood¹⁸ among others¹⁹. A recent study using
87 high-resolution mass spectrometry revealed that the molecular composition of Hg binding
88 dissolved organic matter (DOM) released by green algae *Chlorella vulgaris*, *Chlamydomonas*
89 *reinhardtii* and *Scenedesmus obliquus* depended on natural variation in light intensity and other
90 physicochemical parameters²⁰.

91 Isotopically labelled Hg species were employed for the identification of iHg and MeHg binding
92 affinities to biomolecules in living aquatic organisms²¹. But also, their localization in different cell
93 compartments in methylating and non-methylating sulfate reducing bacteria was achieved¹⁵. In this
94 previous work, the combination of Hg enriched isotopes with gas chromatography (GC)/LC-ICP-
95 MS demonstrated that HMW bioligands released from a methylating strain were exclusively bound
96 to MeHg, however, no structural characterization was provided. The identification of Hg binding
97 HMW proteins requires several purification steps in order to characterize the target protein²².

98 The existing literature of Hg biocomplexes characterization in aquatic microorganisms is limited
99 in terms of molecular mass spectrometry characterization. Using X-ray absorption spectroscopy
100 high energy resolution fluorescence detected X ray absorption near edge structure (XAS-HERFD-
101 XANES or HR-XANES), several Hg species were identified inside biological cells²³⁻²⁵. But also,
102 X-ray absorption spectroscopy fine structure (EXAFS) can be used to elucidate the structural
103 characterization of thiol functional groups among others (O/N) binding iHg^{26,27}.

104 In this work, the study of intracellular complexation of Hg species was carried out by taking
105 advantage of the tracking with isotopically enriched isotopes at low Hg concentration (3 nM / 600
106 ng L⁻¹ ¹⁹⁹iHg & 0.3 nM / 60 ng L⁻¹ Me²⁰¹Hg), one of the lowest reported so far for Hg species

107 incubation with photosynthetic unicellular organisms. The enriched isotopic tracers (^{199}iHg and
108 Me^{201}Hg) were added after cells resuspension in the exposure medium with the purpose of tracing
109 the newly formed Hg biocomplexes in the cytosolic fraction. The main aim of this research was to
110 characterize Hg-biocomplexes involved in Hg speciation and to study different Hg species specific
111 binding affinities at two different growth phases in the intracellular fraction of the cyanobacterium
112 *Synechocystis* sp. PCC 6803. This model cyanobacterium is representative from freshwater
113 ecosystems, a prokaryotic cell with a single chromosome free in cytoplasm and capable of growth
114 by oxygenic photosynthesis or by glycolysis and oxidative phosphorylation in dark conditions; a
115 phytoplankton microorganism structurally and metabolically more similar to bacteria than an
116 eukaryotic cell that can be found in microbial and phytoplankton communities^{28,29}. Then, the
117 combination of complementary information obtained by hyphenated analytical techniques such as
118 GC-ICP-MS, size exclusion chromatography (SEC) -ICP-MS and HILIC-ICP/ESI-MS provide
119 new insights on the role of intracellular ligands in Hg speciation and intracellular fate in
120 photosynthetic microorganisms.

121

122 MATERIAL AND METHODS.

123 **Reagent and Standards.** All solutions were prepared using ultrapure water (18 M Ω cm,
124 Millipore). All samples and standards were prepared with trace metal grade acid (Fisher Scientific
125 Illkrich, France). Working standard solutions were prepared daily by appropriate dilution of the
126 stock standard solutions in 1% of hydrochloric acid (HCl) and stored at 4 °C until use. ¹⁹⁹Hg-
127 enriched inorganic mercury and ²⁰¹Hg-enriched methylmercury (ISC-Science, Oviedo, Spain)
128 were used as incubation spikes or tracers. ¹⁹⁸Hg-enriched inorganic mercury and ²⁰²Hg-enriched
129 methylmercury were used to quantify the endogenous Hg species (¹⁹⁹iHg and Me²⁰¹Hg) present in
130 the bulk and cytosolic fraction. Hg species were derivatized by using sodium tetraethyl borate
131 (NaBEt₄, Merseburger spezial Chemikalien, Germany). Glutathione standard was purchased from
132 Sigma Aldrich (Saint-Quentin-Fallavier, France). The rabbit liver metallothionein-2 isoform
133 standard was purchased from Enzo life sciences (Villeurbanne, France). Sample flasks were
134 cleaned using three successive baths comprising an ultrasonicator bath during 1 hour in nitric acid
135 (HNO₃) 10% (v/v) (twice) and HCl 10% (v/v) (once).

136

137 Experimental procedure.

138 **Culture conditions:** *Synechocystis* sp. PCC 6803 was purchased from the Pasteur Culture
139 collection of Cyanobacteria (PCC, [https://research.pasteur.fr/en/team/collection-of-](https://research.pasteur.fr/en/team/collection-of-cyanobacteria/)
140 [cyanobacteria/](https://research.pasteur.fr/en/team/collection-of-cyanobacteria/)) and cultivated using modified BG11 medium (sodium nitrate replaced by
141 ammonium nitrate) with illumination values of 130 $\mu\text{E m}^{-2} \text{s}^{-1}$ and illumination regime of 14:10 h
142 (light : dark)³⁰

143 **Sampling procedure:** Cells coming from two different cultures in mid-exponential and stationary
144 growth phases were harvested by centrifugation (1300 g, 15 min, 10 °C). At the exponential phase,

145 the cyanobacterial growth is not limited having a maximal number of growing cells. Contrary, the
146 stationary phase corresponds to a situation in which growth rate and death rate are equal. The
147 number of new cells created is limited by the growth factor and as a result, the rate of cell growth
148 matches the rate of cell death. Under such cellular stress conditions, it has been suggested that
149 specific genetic responses are occurring and that the release of extracellular bioligands could be
150 enhanced^{31,32}.

151 Cells were resuspended in 400 mL of exposure medium (composition in Table S1) to a final cell
152 density (2×10^7 cell mL⁻¹) determined by flow cytometry (Accuri C6, BD Biosciences,
153 Switzerland). Then, 200 mL were used as biotic control to check any possible Hg spike
154 contamination and to measure the Hg background already found in the biological system (Figure
155 S1), while the other 200 mL were spiked with 600 ng and 60 ng of ¹⁹⁹HgCl₂ and Me²⁰¹HgOH per
156 L of exposure media, respectively (3 nM ¹⁹⁹iHg & 0.3 nM Me²⁰¹Hg). An aliquot of 45 mL sample
157 was taken and centrifuged (1300 g, 15 min, 10 °C) at exposure times of 5 min and 24h. Pellets
158 were collected and cells were fractionated to membrane fraction and cytosolic fraction as described
159 below. Three independent cell cultures were carried out and incubated simultaneously with
160 enriched Hg isotopes. The medium was sterile and no contamination occurred with other
161 organisms.

162 **Cell fractionation.** Each pellet aliquot was flash frozen in liquid nitrogen to stop the metabolic
163 activity; subsequently 1.5 mL of Milli-Q water was added to the pellet. An Ultra-Sonicator (Sonics
164 Vibra-cell, 130 W, 20 kHz) step was used for 1 minute at 50% amplitude in order to break the
165 cells. Allowing, through a centrifugation (10000 g, 6 min) in a centrifuge 5417R (Eppendorf), the
166 separation of cytosolic fraction (composed by organelles, heat stable proteins (HSP) and heat
167 denatured proteins (HDP)) and membranes with cells debris³³. Cytosolic fraction samples were

168 divided in aliquots and stored at -80 °C to avoid any possible protein degradation for Hg bioligands
169 analysis. The others were acidified with 3N HNO₃ and stored at 4 °C for the quantification of Hg
170 species. The scheme of the cell fractionation procedure performed for Hg species quantification
171 and the investigation of Hg biocomplexes is displayed in Figure S2.

172 **Analysis of Hg binding biomolecules by SEC/HILIC-ICP-MS and HILIC-ESI-** 173 **MS.**

174 **Instrumentation.** An Agilent 1100 liquid chromatography (Agilent, Wilmington, DE) equipped
175 with a binary HPLC pump, an autosampler, and a diode array detector was used. Also,
176 chromatographic separations were carried out using an Agilent 1100 capillary μ HPLC system
177 (Agilent, Tokyo, Japan). An Agilent inductively coupled plasma mass spectrometer (ICP-MS)
178 7500 ce (Yokogawa Analytical Systems, Tokyo, Japan) served for Hg detection and other metals
179 (Fe, Co, Cu and Zn among others) after liquid chromatography separation. This separation system
180 was also coupled to a linear trap quadrupole (LTQ) Orbitrap Velos mass Spectrometer (Thermo
181 Fisher Scientific, Bremen, Germany) in parallel by means of a heated electrospray ionization
182 source (H ESI II).

183 **Chromatographic separation (SEC and HILIC) conditions.** Hg binding biomolecules from
184 cytosolic fraction were separated in the SuperdexTM 200 HR (10 x 300mm x 13 μ m) (Cytiva life
185 sciences) with an operation range of 10 to 600 kDa and used for a wide screening of such
186 biomolecules. For the analysis of LMW compounds, an aliquot from the cytosol (15 μ L) was
187 diluted with acetonitrile (1:2 v/v) in order to precipitate high molecular weight biomolecules
188 following this procedure^{18,22}, with a subsequent addition of 250 μ g of natural inorganic and
189 methylated Hg per L before the injection in a TSKgel[®] amide 80 column (Sigma Aldrich). The
190 hydrophilic interaction liquid chromatography has the advantage of using a polar mobile phase,

191 being compatible with electrospray ionization and enabling the parallel detection in both analytical
192 instruments. The operating parameters for size exclusion chromatography and hydrophilic
193 interaction liquid chromatography coupled to ICP-MS and ESI-MS analysis are shown in Table
194 S2.

195 To accurately determine the molecular mass range that Hg binding LWM bioligands could be
196 found in the cytosolic fraction (under 16 kDa), a screening was carried out in a SuperdexTM Peptide
197 (Cytiva life sciences) with a separation range between 7 and 0.1 kDa; noticing a match around 0.3
198 kDa fraction with a standard of glutathione (GSH) injected with the same chromatographic settings
199 (Figure S3).

200 We have also examined LMW bioligands binding iHg and MeHg in the extracellular medium.
201 However, the limitations of the experimental setup and the analytical approach did not allow us to
202 detect any bioligand binding Hg by SEC-ICPMS in the extracellular medium even after 24 hours
203 of Hg exposure.

204 **Hg species quantification.**

205 **Instrumentation.** A Thermo Electron GC (Trace) coupled to a Thermo Electron ICP-MS (X7 X
206 series) was used for the determination of total concentration of each Hg species.

207 **Sample preparation.** The bulk and cytosolic fraction were digested with 3N HNO₃ under an
208 analytical microwave (Discover and Explorer SP-D 80 system, CEM, NC USA) and analyzed by
209 gas chromatography coupled to inductively coupled plasma mass spectrometry (GC-ICP-MS) as
210 detailed elsewhere³⁴. Before starting the analytical procedure, a certain amount of both enriched
211 spikes in ¹⁹⁸iHg and Me²⁰²Hg, previously characterized in terms of isotopic abundances and
212 concentration, were added to the vial containing the sample. After, 5 mL of an acetic acid/acetate
213 buffer (0.1 M, pH 3.9) were aggregated with a pH adjustment to 3.9. Subsequently, Hg species

214 (endogenous and exogenous) were ethylated using NaBrEt₄ (5% v/v) and extracted in isooctane
215 by automatic shaking for 20 minutes on elliptic table. Quantification of isotopically enriched
216 ¹⁹⁹iHg and Me²⁰¹Hg was carried out by applying double-double isotope dilution analysis based on
217 isotopic pattern deconvolution.

218 **Analytical procedure.** The measurement of the isotopic composition of Hg enriched isotopes in
219 the samples was carried out by GC-ICP-MS. Integration of the chromatographic peaks was carried
220 out using the commercial software Thermo Plasma Lab. The methodological detection limit for
221 iHg and MeHg were 0.05 and 0.03 ng L⁻¹ respectively. All operating parameters for the GC-ICP-
222 MS analysis are found in Table S3. Details of the mathematical approach for quantification of the
223 samples by double-double isotope dilution analysis are observed in Figure S4.

224

225 **RESULTS and DISCUSSION.**

226 **Hg species concentration in the cytosolic fraction.**

227 The concentration of ^{199}iHg and Me^{201}Hg in the bulk (exposure medium and cells) and cytosolic
228 fraction of *Synechosystis* sp. PCC 6803 are presented in Table 1. Overall, similar Hg distribution
229 was observed in exponential and stationary phase. The proportion of ^{199}iHg and Me^{201}Hg in the
230 cytosolic fraction ranged between 9-10 % and 32-36 % respectively after 24 hours of Hg exposure
231 at both growth phases. At the beginning ($t=5\text{min}$), the concentration of ^{199}iHg ranged between 6-8
232 ng L^{-1} whereas, for Me^{201}Hg ranged between 13-19 ng L^{-1} in the cytosolic fraction. No large
233 distinctions were found for Me^{201}Hg after 24 hours whereas, a higher uptake of ^{199}iHg was
234 observed at both growth phases.

235

236

237

238

239

240

241

242

243

244

245

246

247

248 **Table 1.** ^{199}iHg and Me^{201}Hg species proportion and concentration (ng L^{-1}) in the bulk (exposure medium
 249 and cells) and cytosolic fraction in the beginning (5min) and after 24h exposure of *Synechocystis* sp. PCC
 250 6803 in exponential and stationary growth phases. Mean \pm sd (n=3).

251

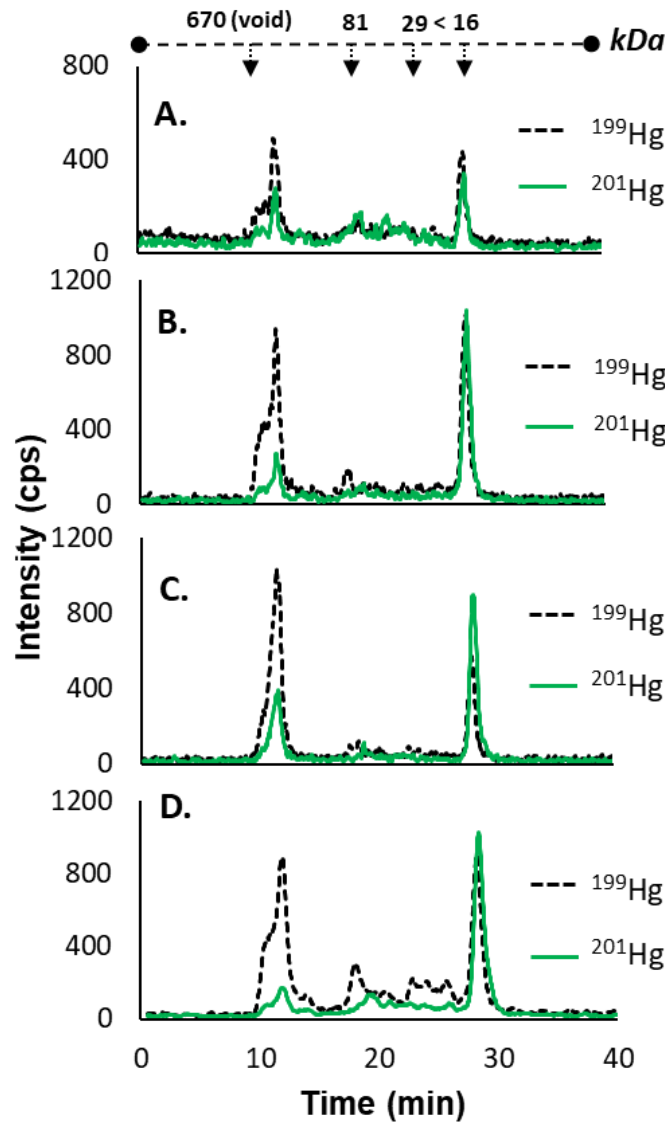
252

<i>Exponential</i> <i>phase</i>	^{199}iHg		Me^{201}Hg	
	$t_{5\text{min}}$	$t_{24\text{h}}$	$t_{5\text{min}}$	$t_{24\text{h}}$
Bulk (ng L^{-1})	517 \pm 14	379 \pm 24	52 \pm 1	47 \pm 3
Cytosolic fraction (ng L^{-1})	6 \pm 1	35 \pm 9	13 \pm 1	15 \pm 2
Cytosolic fraction vs Bulk (%)	1.2 \pm 0.2	9.2 \pm 2.4	25 \pm 2	32 \pm 4

<i>Stationary</i> <i>phase</i>	^{199}iHg		Me^{201}Hg	
	$t_{5\text{min}}$	$t_{24\text{h}}$	$t_{5\text{min}}$	$t_{24\text{h}}$
Bulk (ng L^{-1})	549 \pm 28	421 \pm 23	54 \pm 1	50 \pm 1
Cytosolic fraction (ng L^{-1})	8 \pm 3	41 \pm 7	19 \pm 1	18 \pm 1
Cytosolic fraction vs Bulk (%)	1.5 \pm 0.5	9.7 \pm 1.7	35 \pm 2	36 \pm 2

253 Hg binding bioligands screening in the cytosolic fraction.

254



255

256 **Figure 1.** Size exclusion chromatograms (Superdex 200 (Range: 600 - 10 kDa)) in the cytosolic fraction of

257 *Synechocystis* sp. PCC 6803 by ICP-MS detection of (A) ^{199}Hg and ^{201}Hg corresponding to both Hg isotopic

258 tracers (^{199}iHg and Me^{201}Hg) after 5 minutes of exposure in the exponential phase. (B) ^{199}Hg and ^{201}Hg

259 corresponding to both isotopic tracers (^{199}iHg and Me^{201}Hg) after 24 hours of exposure in the exponential

260 phase. (C) ^{199}Hg and ^{201}Hg corresponding to both Hg isotopic tracers (^{199}iHg and Me^{201}Hg) after 5 minutes

261 of exposure in the stationary phase. (D) ^{199}Hg and ^{201}Hg corresponding to both isotopic tracers (^{199}iHg and
 262 Me^{201}Hg) after 24 hours of exposure in the stationary phase.

263
 264 The analysis by SEC-ICP-MS of the cytosolic fraction reveals two main Hg-containing fractions
 265 with HMW (≥ 600 kDa, 10-13 min) and LMW (≤ 16 kDa, 27-29 min) in a range from 600 to 10
 266 kDa (Figure 1). The increase of ^{199}Hg signal was correlated with the exposure time from 5 min to
 267 24h. ^{199}iHg was preferentially bound to HMW biomolecules eluting around 10-13 min at the
 268 beginning of the Hg exposure. After 24 hours, the intensity of ^{199}iHg binding HMW fraction (≥ 600
 269 kDa) remained constant whereas, a remarkable increase in ^{199}Hg intensity was seen at longer
 270 elution time corresponding to fractions of lower molecular weight; from 29 to 81 kDa (17-26 min)
 271 and under 16 kDa (27-29 min). On the other hand, Me^{201}Hg was mostly bound to LMW fraction
 272 exhibiting an intensity increase after 24h exposure at both growth phases.

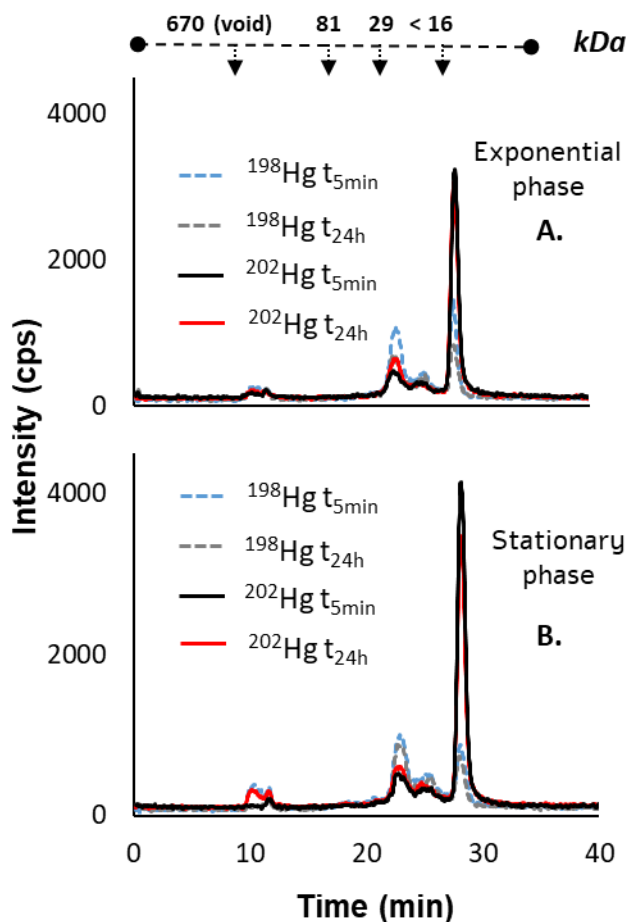
273 Despite SEC-ICP-MS analysis does not give quantitative information, we have estimated the
 274 proportion of ^{199}iHg and Me^{201}Hg bound to LMW cytosolic ligands (Table 2) based on the peak
 275 area of eluted compounds (Figure 1).

276 **Table 2.** Percentage of ^{199}iHg and Me^{201}Hg bound to LMW fraction of cytosolic ligands at the beginning
 277 and after 24h exposure at different growth phases in *Synechocystis* sp. PCC 6803. Mean \pm sd (n=3).

% Hg binding LMW fraction	^{199}iHg		Me^{201}Hg	
	$t_{5\text{min}}$	$t_{24\text{h}}$	$t_{5\text{min}}$	$t_{24\text{h}}$
Exponential phase	38 \pm 8 %	47 \pm 11 %	68 \pm 5%	79 \pm 4%
Stationary phase	35 \pm 14 %	46 \pm 8 %	67 \pm 4%	86 \pm 9 %

278
 279 Table 2 shows the percentage of Hg bound to the LMW fraction at the beginning and after 24
 280 hours of Hg exposure at different growth phases in which the proportion of ^{199}iHg and Me^{201}Hg

281 bound to the LMW fraction after 24 hours of Hg exposure were 46-47 % and 79-86 % respectively,
282 at both growth phases.
283 To obtain further information about the specificity and affinity of Hg to bioligands, two different
284 enriched Hg species (^{198}iHg and Me^{202}Hg) were subsequently added to the cytosolic fraction that
285 had been previously exposed to ^{199}iHg and Me^{201}Hg (Figure 2).



286
287 **Figure 2.** Size exclusion chromatograms (Superdex 200 (Range: 600-10 KDa)) in the cytosolic fraction of
288 *Synechocystis* sp. PCC 6803 in the exponential (A) and stationary growth phase (B) by ICP-MS detection
289 of ^{198}Hg and ^{202}Hg corresponding to the addition ($5 \mu\text{g L}^{-1}$) of ^{198}iHg and Me^{202}Hg after 5 minutes and 24
290 hours of Hg exposure of both isotopic tracers (^{199}iHg and Me^{201}Hg).
291

292 The obtained results in figure 2 evidenced similar patterns to endogenous Hg biocomplexes
293 distribution from figure 1 confirming the specific affinity of LMW fraction (27-29 min) for MeHg.
294 But also, it demonstrates that bioligands functional groups in the LMW fraction are still available
295 to bind iHg and MeHg.

296 Overall, the transition from exponential to stationary growth phase involves several adaptations
297 such as changes in proteins expression involved in cell growth, protein biosynthesis involved in
298 nutrient uptake and proteins related to energy metabolism^{32,35}. Nutrient availability is the main
299 critical factor that determines the growth phase changes. In the existing literature, no studies have
300 ever reported comparisons in the distribution of iHg or MeHg binding intracellular ligands between
301 exponential and stationary phase in phytoplankton. Under our experimental conditions, the
302 differences in Hg exposure time or growth phase have not affected the distribution of potential
303 bioligands capable of binding exogenous Hg. This result is important to highlight since the amount
304 of the extracellular ligands released at the stationary phase could be higher³¹ and was expected to
305 influence the amount of the bioaccumulated iHg or MeHg.

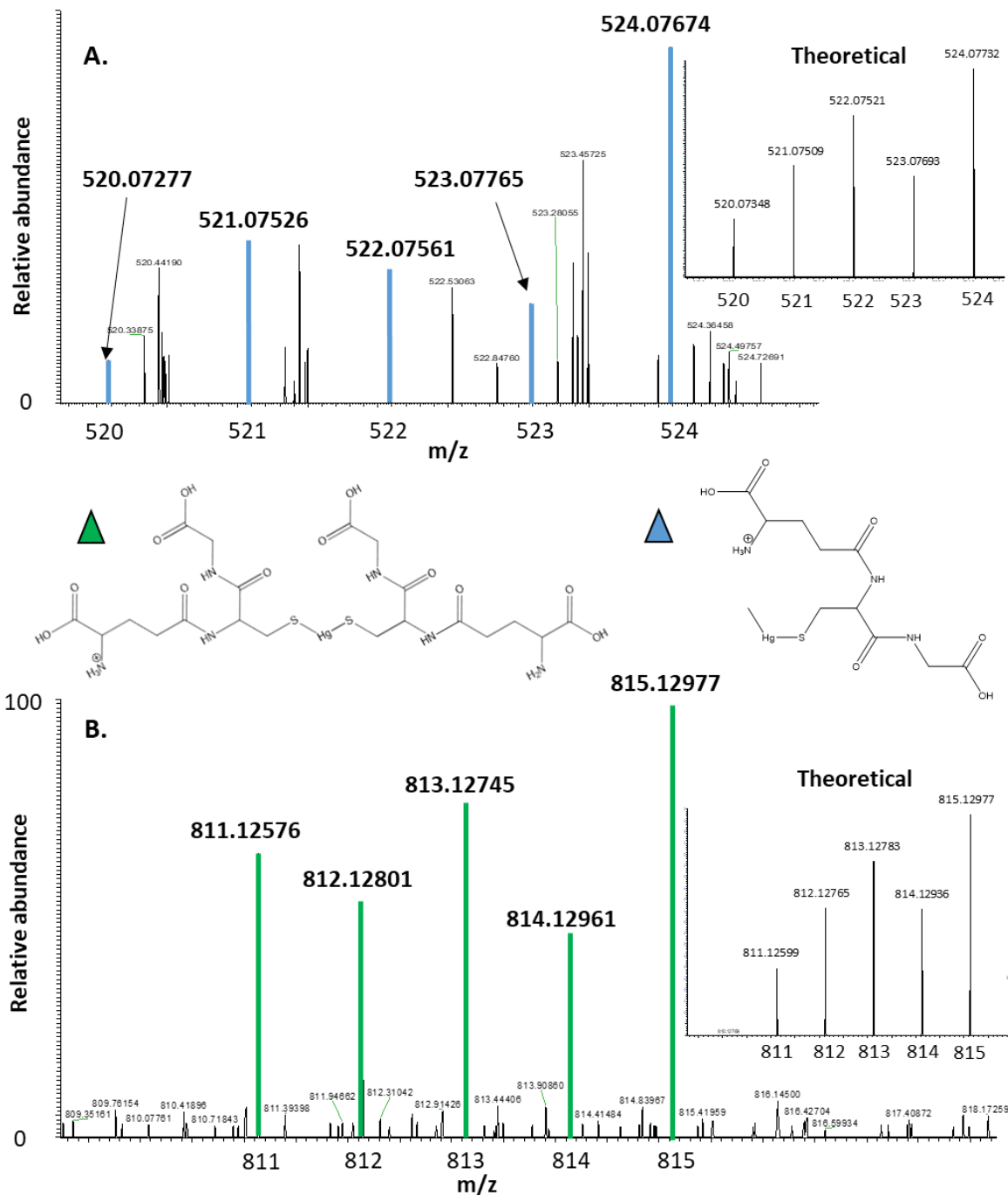
306 Understanding of iHg and MeHg intracellular fate is a key factor to explain the role of the
307 intracellular bioligands in Hg speciation. In our work, the increase of the signal intensity of ¹⁹⁹iHg
308 and Me²⁰¹Hg bound to the LMW fraction (< 16 kDa) after 24 h in the stationary phase suggests
309 that these specific biomolecules, where heat stable proteins among others are present, could be
310 involved in Hg species specific sequestration at nontoxic levels. This falls in agreement with recent
311 observations of the synthesis of glutathione and PCs by a marine diatom *Thalassiosira weissflogii*
312 when exposed to iHg and MeHg^{36,37}. Furthermore, the findings concerning the species specific
313 affinity of iHg binding HMW fraction and MeHg binding LMW fraction agree with a previous
314 study carried out with three marine phytoplankton (*Thalassiosira pseudonana*, *Chlorella*

315 *autotrophica* and *Isochrysis galbana*), where heat stable proteins were mainly binding MeHg
316 whereas iHg was associated to the organelles fraction³⁸. However, these experiments are not
317 directly comparable since higher Hg concentrations were added in comparison with our work (>
318 150 folds for iHg).

319 Although the specific function of these biogenic intracellular ligands cannot be clarified with the
320 available data, the Hg binding bioligands detected may also be involved in several Hg
321 transformations such as biotic reduction or biotic demethylation^{39,40}. It should be noticed that so
322 far only two studies reported the use of simultaneous enriched isotopes for iHg and MeHg in cell
323 culture experiments. On one hand, to investigate the Hg species accumulation and biotic
324 transformations in *C. reinhardtii*³⁹ and on the other hand, to explore the Hg biocomplexes
325 distribution size in the extracellular and intracellular fraction in methylating and non methylating
326 sulfate-reducing bacteria¹⁵. Nevertheless, no structural characterization of Hg biocomplexes was
327 provided. Additionally, most of the studies focused on the intracellular compartment of
328 phytoplankton cell cultures have been carried out under high Hg exposure concentrations (1000-
329 10000 higher than our conditions), in order to study the Hg accumulation, subcellular distribution
330 and detoxification mechanisms³⁸⁻⁴². On the contrary, our work used lower Hg concentrations of 3
331 nM / 600 ng L⁻¹ for ¹⁹⁹iHg and 0.3 nM / 60 ng L⁻¹ for Me²⁰¹Hg. Therefore, it is not expected to
332 have induced considerable physiological changes in the main intracellular processes^{43,44}.
333 Additionally, other essential elements (Cu, Zn, Fe and Co) were monitored by SEC-ICP-MS. In
334 this case, cells that were exposed to Hg did not induce the formation of new metal-biocomplexes
335 fractions in their SEC chromatogram profiles (Figure S5) comparing with the biotic controls (no
336 Hg exposure).

337 **Identification of intracellular Hg species-specific biogenic complexes in the low molecular**
338 **weight fraction.**

339 The identification of biomolecules is usually based on the retention time matching of standards
340 and samples. However, the structural characterization provides an unambiguous identification of
341 the molecular structure, representing a step further in terms of Hg biocomplexes determination.



342
 343 **Figure 3. (A)** Zoom of the mass spectra obtained at 21.2 min demonstrates the presence of MeHg binding
 344 one glutathione with its natural Hg isotopic pattern (^{202}Hg m/z = 524.08). **(B).** Zoom of the mass spectra
 345 obtained at 23.5 min demonstrate the presence of Hg binding two glutathione with its natural Hg isotopic
 346 pattern in stationary phase (^{202}Hg m/z = 815.13).

347 The analysis by HILIC-ICP-MS of the cytosolic fraction reveals two Hg binding bioligands
348 corresponding to two different peaks with specific retention times at 21.0 min and 23.7 min (Figure
349 S6A) based on Hg isotopes monitoring (elemental ionization). For this purpose, the injection of
350 the same cytosolic fraction carrying out the same chromatographic settings (leading to matching
351 retention times) was done by coupling to an electrospray ionization mass spectrometer and
352 providing structural information about the compounds previously detected (Figure S6B). Firstly,
353 the natural isotopic pattern of Hg was investigated in the full scan spectra at both retention times.
354 Electrospray MS at the retention time of first peak revealed one ion with the isotopic pattern of
355 mercury (Figure 3A) at $m/z = 524.08$ (m/z corresponding to the most abundant isotope in the
356 isotopic distribution). This mass to charge ratio corresponded to Hg methylated binding one
357 glutathione (GS-MeHg, $C_{11}H_{20}HgN_3O_6S^+$). Regarding the second peak, the Hg isotopic pattern
358 was observed (Figure 3B) at $m/z = 815.13$ corresponding to iHg binding two glutathione ((GS)₂-
359 Hg), $C_{20}H_{33}HgN_6O_{12}S_2^+$). Even if the theoretical natural isotopic pattern for iHg and MeHg binding
360 glutathione did not match in all isotopes in comparison with the experimental Hg isotopic patterns,
361 caused by the low concentration of iHg and MeHg bound to GSH, the experimental masses agreed
362 with the theoretical ones.

363 The present results confirmed that GSH is playing a key role in Hg sequestration in different
364 aquatic microorganisms^{37,45}. Particularly in cyanobacteria, GSH plays a central role in redox
365 control of protein thiols and disulfide bonds, including protection against toxic metabolites,
366 xenobiotic and oxidative stress^{46,47}. Hg exposure is well known to induce accumulation of reactive
367 oxygen species and peroxidation products in phytoplankton⁴³. Under oxidative stress, glutathione
368 acts as a protein reductant against highly reactive oxidants such as singlet oxygen, superoxide and
369 hydroxyl radicals forming GS-SG²⁹. Nevertheless, the reduction of GS-SG (S-S) to two GSH is

370 mediated by the enzyme glutathione reductase being a critical process for its regeneration.
371 Exposure of green alga *Chlamydomonas reinhardtii* to sub-toxic concentrations of iHg and MeHg
372 resulted in a significant increase of reduced glutathione after Hg-treatments⁴⁴. GSH is a precursor
373 of phytochelatins synthesis, which can be activated following the exposure to different toxic metals
374 including Hg⁴⁴. The cyanobacterial phytochelatin synthesis was shown to be close functionally to
375 that of plants. Additionally, the phytochelatin synthase exhibited transpeptidasic activity during
376 Cd- exposure, being able to synthesize phytochelatins with a degree of oligomerization higher than
377 PC₂⁴⁸. Furthermore, Hg exposure induced changes in intracellular thiols concentration such as
378 glutathione or phytochelatins demonstrating that algae can control the intracellular Hg
379 speciation^{36,37,40}. Phytoplankton intracellular detoxification mechanisms can promote the
380 transformation of iHg into gaseous Hg^{37,49}. In bacteria, it was shown that the intracellular
381 reduction is carried out enzymatically⁵⁰.

382 In the extracellular fraction, several studies have demonstrated the influence of LMW bioligands
383 on Hg speciation^{51,52}. Particularly, high rates of iHg uptake and biotic methylation were observed
384 in the presence of some complexing LMW thiols such as cysteine whereas, GSH inhibited these
385 processes⁵². These results suggest that the molecular structure of the bioligands plays a crucial role
386 in Hg speciation in anaerobic environments. Additional information was obtained in a freshwater
387 green microalga *Selenastrum capricornutum*⁸. Skrobonja et al. 2019 showed that the
388 thermodynamic stability in turns with the chemical structure of MeHg LMW complexes in the
389 extracellular medium govern the rate of MeHg interactions with the cell surface⁸. Further
390 investigations must be carried out to explore the role of these intra- and extra-cellular ligands in
391 Hg speciation but also, structural studies based on molecular mass spectrometry will be needed to
392 elucidate the exact function of the biomolecules involved in Hg speciation.

393 **Environmental perspective.**

394 The identification of glutathione as a bioligand binding to iHg ((GS)₂-Hg) and MeHg (GS-MeHg)
395 in cyanobacterium *Synechocystis* sp. PCC 6803 has demonstrated that glutathione plays an
396 important role in Hg intracellular handling; reducing probably the potential damage that both Hg
397 species could cause on the cellular metabolism. In aquatic environment, cyanobacteria are found
398 in various environmental settings interacting with different aquatic microorganisms with a specific
399 role into the natural Hg cycle. The pioneering approach based on the combination of enriched
400 isotopes and mass spectrometry techniques represent a first step, towards explaining and
401 understanding the intracellular speciation of iHg and MeHg in photosynthetic microorganisms.
402 Important emphasis should be placed concerning to global warming and/or water pollution⁵³.
403 Particularly, cyanobacteria are considered to prevail in warmer freshwaters and their proportion
404 will increase in phytoplankton communities⁵⁴. Cyanobacteria are more resistant to pollutant
405 exposure, high temperatures and eutrophication events caused by the global warming or nutrient
406 contamination than other phytoplankton species^{55,56}. Furthermore, phytoplankton communities are
407 the main entry point in the trophic transfer for Hg. For these reasons, our results exemplify the
408 potential bioaccumulation of iHg and MeHg at non toxic levels by a model phytoplankton.

409

410 **Notes**

411 **The authors declare no competing financial interest.**

412 **ACKNOWLEDGMENTS**

413 Financial support from Agence National de la Recherche (ARN) (Project-ANR-17-CE34-0014)
414 and Swiss National Science Foundation (SNF) (project N 175721) in the framework of the
415 PHYTAMBA project (PRCI ANR/SNSF). Financial support from E2S/UPPA (Energy and

416 Environment Solutions) in the framework of the MESMIC Hub (Metals in Environmental System
417 Microbiology).

418

419 REFERENCES

- 420 (1) Zhang, J.; Wang, F.; House, J. D.; Page, B. Thiols in Wetland Interstitial Waters and Their
421 Role in Mercury and Methylmercury Speciation. *Limnology and Oceanography* **2004**, *49*
422 (6), 2276–2286. <https://doi.org/10.4319/lo.2004.49.6.2276>.
- 423 (2) Liem-Nguyen, V.; Bouchet, S.; Björn, E. Determination of Sub-Nanomolar Levels of Low
424 Molecular Mass Thiols in Natural Waters by Liquid Chromatography Tandem Mass
425 Spectrometry after Derivatization with p-(Hydroxymercuri) Benzoate and Online
426 Preconcentration. *Anal. Chem.* **2015**, *87* (2), 1089–1096.
427 <https://doi.org/10.1021/ac503679y>.
- 428 (3) Bouchet, S.; Goñi-Urriza, M.; Monperrus, M.; Guyoneaud, R.; Fernandez, P.; Heredia, C.;
429 Tessier, E.; Gassie, C.; Point, D.; Guédron, S.; Achá, D.; Amouroux, D. Linking Microbial
430 Activities and Low-Molecular-Weight Thiols to Hg Methylation in Biofilms and Periphyton
431 from High-Altitude Tropical Lakes in the Bolivian Altiplano. *Environmental Science &*
432 *Technology* **2018**, *52* (17), 9758–9767. <https://doi.org/10.1021/acs.est.8b01885>.
- 433 (4) Liem-Nguyen, V.; Huynh, K.; Gallampois, C.; Björn, E. Determination of Picomolar
434 Concentrations of Thiol Compounds in Natural Waters and Biological Samples by Tandem
435 Mass Spectrometry with Online Preconcentration and Isotope-Labeling Derivatization.
436 *Analytica Chimica Acta* **2019**, *1067*, 71–78. <https://doi.org/10.1016/j.jaca.2019.03.035>.
- 437 (5) Leclerc, M.; Planas, D.; Amyot, M. Relationship between Extracellular Low-Molecular-
438 Weight Thiols and Mercury Species in Natural Lake Periphytic Biofilms. *Environmental*
439 *Science & Technology* **2015**, *49* (13), 7709–7716. <https://doi.org/10.1021/es505952x>.
- 440 (6) Kuśmierk, K.; Chwatko, G.; Głowacki, R.; Kubalczyk, P.; Bald, E. Ultraviolet
441 Derivatization of Low-Molecular-Mass Thiols for High Performance Liquid
442 Chromatography and Capillary Electrophoresis Analysis. *Journal of Chromatography B*
443 **2011**, *879* (17–18), 1290–1307. <https://doi.org/10.1016/j.jchromb.2010.10.035>.
- 444 (7) G. Berthon. The Stability Constants of Metal Complexes of Amino Acids with Polar Side
445 Chains. *Pure & Appl. Chem.* **1995**, *69*, 1117–1240.
446 <https://doi.org/10.1351/PAC199567071117>.
- 447 (8) Skrobonja, A.; Gojkovic, Z.; Soerensen, A. L.; Westlund, P.-O.; Funk, C.; Björn, E. Uptake
448 Kinetics of Methylmercury in a Freshwater Alga Exposed to Methylmercury Complexes
449 with Environmentally Relevant Thiols. *Environ. Sci. Technol.* **2019**, *acs.est.9b05164*.
450 <https://doi.org/10.1021/acs.est.9b05164>.
- 451 (9) Liem-Nguyen, V.; Nguyen-Ngoc, H.-T.; Adediran, G. A.; Björn, E. Determination of
452 Picomolar Levels of Methylmercury Complexes with Low Molecular Mass Thiols by
453 Liquid Chromatography Tandem Mass Spectrometry and Online Preconcentration. *Anal*
454 *Bioanal Chem* **2020**. <https://doi.org/10.1007/s00216-020-02389-y>.
- 455 (10) Monperrus, M.; Tessier, E.; Amouroux, D.; Leynaert, A.; Huonnic, P.; Donard, O. F. X.
456 Mercury Methylation, Demethylation and Reduction Rates in Coastal and Marine Surface

- 457 Waters of the Mediterranean Sea. *Marine Chemistry* **2007**, *107* (1), 49–63.
458 <https://doi.org/10.1016/j.marchem.2007.01.018>.
- 459 (11) Lalonde, J. D.; Amyot, M.; Kraepiel, A. M. L.; Morel, F. M. M. Photooxidation of Hg(0) in
460 Artificial and Natural Waters. *Environmental Science & Technology* **2001**, *35* (7), 1367–
461 1372. <https://doi.org/10.1021/es001408z>.
- 462 (12) Celo, V.; Lean, D. R. S.; Scott, S. L. Abiotic Methylation of Mercury in the Aquatic
463 Environment. *Science of The Total Environment* **2006**, *368* (1), 126–137.
464 <https://doi.org/10.1016/j.scitotenv.2005.09.043>.
- 465 (13) Grégoire, D. S.; Poulain, A. J. A Little Bit of Light Goes a Long Way: The Role of
466 Phototrophs on Mercury Cycling. *Metallomics* **2014**, *6* (3), 396.
467 <https://doi.org/10.1039/c3mt00312d>.
- 468 (14) Le Faucheur, S.; Campbell, P. G. C.; Fortin, C.; Slaveykova, V. I. Interactions between
469 Mercury and Phytoplankton: Speciation, Bioavailability, and Internal Handling: Mercury-
470 Phytoplankton Interactions. *Environmental Toxicology and Chemistry* **2014**, *33* (6), 1211–
471 1224. <https://doi.org/10.1002/etc.2424>.
- 472 (15) Pedrero, Z.; Bridou, R.; Mounicou, S.; Guyoneaud, R.; Monperrus, M.; Amouroux, D.
473 Transformation, Localization, and Biomolecular Binding of Hg Species at Subcellular Level
474 in Methylating and Nonmethylating Sulfate-Reducing Bacteria. *Environmental Science &*
475 *Technology* **2012**, *46* (21), 11744–11751. <https://doi.org/10.1021/es302412q>.
- 476 (16) Krupp, E. M.; Milne, B. F.; Mestrot, A.; Meharg, A. A.; Feldmann, J. Investigation into
477 Mercury Bound to Biothiols: Structural Identification Using ESI–Ion-Trap MS and
478 Introduction of a Method for Their HPLC Separation with Simultaneous Detection by ICP-
479 MS and ESI-MS. *Anal Bioanal Chem* **2008**, *390* (7), 1753–1764.
480 <https://doi.org/10.1007/s00216-008-1927-x>.
- 481 (17) Pedrero, Z.; Ouerdane, L.; Mounicou, S.; Lobinski, R.; Monperrus, M.; Amouroux, D.
482 Identification of Mercury and Other Metals Complexes with Metallothioneins in Dolphin
483 Liver by Hydrophilic Interaction Liquid Chromatography with the Parallel Detection by ICP
484 MS and Electrospray Hybrid Linear/Orbital Trap MS/MS. *Metallomics* **2012**, *4* (5), 473.
485 <https://doi.org/10.1039/c2mt00006g>.
- 486 (18) Klein, M.; Ouerdane, L.; Bueno, M.; Pannier, F. Identification in Human Urine and Blood
487 of a Novel Selenium Metabolite, Se-Methylselenoneine, a Potential Biomarker of
488 Metabolization in Mammals of the Naturally Occurring Selenoneine, by HPLC Coupled to
489 Electrospray Hybrid Linear Ion Trap-Orbital Ion Trap MS. *Metallomics* **2011**, *3* (5), 513.
490 <https://doi.org/10.1039/c0mt00060d>.
- 491 (19) Trümpler, S.; Lohmann, W.; Meermann, B.; Buscher, W.; Sperling, M.; Karst, U.
492 Interaction of Thimerosal with Proteins—Ethylmercuryadduct Formation of Human Serum
493 Albumin and β -Lactoglobulin A. *Metallomics* **2009**, *1* (1), 87–91.
494 <https://doi.org/10.1039/B815978E>.
- 495 (20) Mangal, V.; Phung, T.; Nguyen, T. Q.; Guéguen, C. Molecular Characterization of Mercury
496 Binding Ligands Released by Freshwater Algae Grown at Three Photoperiods. *Front.*
497 *Environ. Sci.* **2019**, *6*. <https://doi.org/10.3389/fenvs.2018.00155>.
- 498 (21) Pedrero, Z.; Mounicou, S.; Monperrus, M.; Amouroux, D. Investigation of Hg Species
499 Binding Biomolecules in Dolphin Liver Combining GC and LC-ICP-MS with Isotopic
500 Tracers. *J. Anal. At. Spectrom.* **2011**, *26* (1), 187–194. <https://doi.org/10.1039/C0JA00154F>.
- 501 (22) Pedrero Zayas, Z.; Ouerdane, L.; Mounicou, S.; Lobinski, R.; Monperrus, M.; Amouroux,
502 D. Hemoglobin as a Major Binding Protein for Methylmercury in White-Sided Dolphin

- 503 Liver. *Anal Bioanal Chem* **2014**, *406* (4), 1121–1129. [https://doi.org/10.1007/s00216-013-](https://doi.org/10.1007/s00216-013-7274-6)
504 7274-6.
- 505 (23) Manceau, A.; Nagy, K. L.; Glatzel, P.; Bourdineaud, J.-P. Acute Toxicity of Divalent
506 Mercury to Bacteria Explained by the Formation of Dicysteinate and Tetracysteinate
507 Complexes Bound to Proteins in *Escherichia Coli* and *Bacillus Subtilis*. *Environ. Sci.*
508 *Technol.* **2021**, *55* (6), 3612–3623. <https://doi.org/10.1021/acs.est.0c05202>.
- 509 (24) Manceau, A.; Azemard, S.; Hédouin, L.; Vassileva, E.; Lecchini, D.; Fauvelot, C.;
510 Swarzenski, P. W.; Glatzel, P.; Bustamante, P.; Metian, M. Chemical Forms of Mercury in
511 Blue Marlin Billfish: Implications for Human Exposure. *Environ. Sci. Technol. Lett.* **2021**,
512 *8* (5), 405–411. <https://doi.org/10.1021/acs.estlett.1c00217>.
- 513 (25) Manceau, A.; Gaillot, A.-C.; Glatzel, P.; Cherel, Y.; Bustamante, P. In Vivo Formation of
514 HgSe Nanoparticles and Hg–Tetrarselenolate Complex from Methylmercury in Seabirds—
515 Implications for the Hg–Se Antagonism. *Environ. Sci. Technol.* **2021**, *55* (3), 1515–1526.
516 <https://doi.org/10.1021/acs.est.0c06269>.
- 517 (26) Song, Y.; Adediran, G. A.; Jiang, T.; Hayama, S.; Björn, E.; Skyllberg, U. Toward an
518 Internally Consistent Model for Hg(II) Chemical Speciation Calculations in Bacterium–
519 Natural Organic Matter–Low Molecular Mass Thiol Systems. *Environ. Sci. Technol.* **2020**,
520 *54* (13), 8094–8103. <https://doi.org/10.1021/acs.est.0c01751>.
- 521 (27) Song, Y.; Jiang, T.; Liem-Nguyen, V.; Sparrman, T.; Björn, E.; Skyllberg, U.
522 Thermodynamics of Hg(II) Bonding to Thiol Groups in Suwannee River Natural Organic
523 Matter Resolved by Competitive Ligand Exchange, Hg L_{III}-Edge EXAFS and ¹H NMR
524 Spectroscopy. *Environ. Sci. Technol.* **2018**, *52* (15), 8292–8301.
525 <https://doi.org/10.1021/acs.est.8b00919>.
- 526 (28) Liberton, M.; Page, L. E.; O’Dell, W. B.; O’Neill, H.; Mamontov, E.; Urban, V. S.; Pakrasi,
527 H. B. Organization and Flexibility of Cyanobacterial Thylakoid Membranes Examined by
528 Neutron Scattering. *J. Biol. Chem.* **2013**, *288* (5), 3632–3640.
529 <https://doi.org/10.1074/jbc.M112.416933>.
- 530 (29) Sarma, T. A. *Handbook of Cyanobacteria*, 0 ed.; CRC Press, 2012.
531 <https://doi.org/10.1201/b14316>.
- 532 (30) Stanier, R. Y.; Deruelles, J.; Rippka, R.; Herdman, M.; Waterbury, J. B. Generic
533 Assignments, Strain Histories and Properties of Pure Cultures of Cyanobacteria. *Journal of*
534 *General Microbiology* **1979**, *111* (1), 1–61. <https://doi.org/10.1099/00221287-111-1-1>.
- 535 (31) Jaishankar, J.; Srivastava, P. Molecular Basis of Stationary Phase Survival and
536 Applications. *Front. Microbiol.* **2017**, *8*, 2000. <https://doi.org/10.3389/fmicb.2017.02000>.
- 537 (32) Muthusamy, S.; Lundin, D.; Branca, R. M. M.; Baltar, F.; González, J. M.; Lehtiö, J.;
538 Pinhassi, J. Comparative Proteomics Reveals Signature Metabolisms of Exponentially
539 Growing and Stationary Phase Marine Bacteria. *Environmental Microbiology* **2017**, *19* (6),
540 2301–2319. <https://doi.org/10.1111/1462-2920.13725>.
- 541 (33) Lavoie, M.; Le Faucheur, S.; Fortin, C.; Campbell, P. G. C. Cadmium Detoxification
542 Strategies in Two Phytoplankton Species: Metal Binding by Newly Synthesized Thiolated
543 Peptides and Metal Sequestration in Granules. *Aquatic Toxicology* **2009**, *92* (2), 65–75.
544 <https://doi.org/10.1016/j.aquatox.2008.12.007>.
- 545 (34) Bridou, R.; Monperrus, M.; Gonzalez, P. R.; Guyoneaud, R.; Amouroux, D. Simultaneous
546 Determination of Mercury Methylation and Demethylation Capacities of Various Sulfate-
547 Reducing Bacteria Using Species-Specific Isotopic Tracers. *Environmental Toxicology and*
548 *Chemistry* **2011**, *30* (2), 337–344. <https://doi.org/10.1002/etc.395>.

- 549 (35) Schuurmans, R. M.; Matthijs, J. C. P.; Hellingwerf, K. J. Transition from Exponential to
550 Linear Photoautotrophic Growth Changes the Physiology of *Synechocystis* Sp. PCC 6803.
551 *Photosynth Res* **2017**, *132* (1), 69–82. <https://doi.org/10.1007/s11120-016-0329-8>.
- 552 (36) Wu, Y.; Wang, W.-X. Thiol Compounds Induction Kinetics in Marine Phytoplankton
553 during and after Mercury Exposure. *Journal of Hazardous Materials* **2012**, *217–218*, 271–
554 278. <https://doi.org/10.1016/j.jhazmat.2012.03.024>.
- 555 (37) Morelli, E.; Ferrara, R.; Bellini, B.; Dini, F.; Di Giuseppe, G.; Fantozzi, L. Changes in the
556 Non-Protein Thiol Pool and Production of Dissolved Gaseous Mercury in the Marine
557 Diatom *Thalassiosira weissflogii* under Mercury Exposure. *Science of The Total*
558 *Environment* **2009**, *408* (2), 286–293. <https://doi.org/10.1016/j.scitotenv.2009.09.047>.
- 559 (38) Wu, Y.; Wang, W.-X. Accumulation, Subcellular Distribution and Toxicity of Inorganic
560 Mercury and Methylmercury in Marine Phytoplankton. *Environmental Pollution* **2011**, *159*
561 (10), 3097–3105. <https://doi.org/10.1016/j.envpol.2011.04.012>.
- 562 (39) Bravo, A. G.; Le Faucheur, S.; Monperrus, M.; Amouroux, D.; Slaveykova, V. I. Species-
563 Specific Isotope Tracers to Study the Accumulation and Biotransformation of Mixtures of
564 Inorganic and Methyl Mercury by the Microalga *Chlamydomonas Reinhardtii*.
565 *Environmental Pollution* **2014**, *192*, 212–215.
566 <https://doi.org/10.1016/j.envpol.2014.05.013>.
- 567 (40) Wu, Y.; Wang, W.-X. Intracellular Speciation and Transformation of Inorganic Mercury in
568 Marine Phytoplankton. *Aquatic Toxicology* **2014**, *148*, 122–129.
569 <https://doi.org/10.1016/j.aquatox.2014.01.005>.
- 570 (41) Pickhardt, P. C.; Fisher, N. S. Accumulation of Inorganic and Methylmercury by Freshwater
571 Phytoplankton in Two Contrasting Water Bodies. *Environ. Sci. Technol.* **2007**, *41* (1), 125–
572 131. <https://doi.org/10.1021/es060966w>.
- 573 (42) Pickhardt, P. C.; Folt, C. L.; Chen, C. Y.; Klaue, B.; Blum, J. D. Impacts of Zooplankton
574 Composition and Algal Enrichment on the Accumulation of Mercury in an Experimental
575 Freshwater Food Web. *Science of The Total Environment* **2005**, *339* (1–3), 89–101.
576 <https://doi.org/10.1016/j.scitotenv.2004.07.025>.
- 577 (43) Elbaz, A.; Wei, Y. Y.; Meng, Q.; Zheng, Q.; Yang, Z. M. Mercury-Induced Oxidative Stress
578 and Impact on Antioxidant Enzymes in *Chlamydomonas Reinhardtii*. *Ecotoxicology* **2010**,
579 *19* (7), 1285–1293. <https://doi.org/10.1007/s10646-010-0514-z>.
- 580 (44) Slaveykova, V. I.; Majumdar, S.; Regier, N.; Li, W.; Keller, A. A. Metabolomic Responses
581 of Green Alga *Chlamydomonas Reinhardtii* Exposed to Sublethal Concentrations of
582 Inorganic and Methylmercury. *Environ. Sci. Technol.* **2021**, *acs.est.0c08416*.
583 <https://doi.org/10.1021/acs.est.0c08416>.
- 584 (45) Devars, S.; Avilés, C.; Cervantes, C.; Moreno-Sánchez, R. Mercury Uptake and Removal
585 by *Euglena Gracilis*. *Archives of Microbiology* **2000**, *174* (3), 175–180.
586 <https://doi.org/10.1007/s002030000193>.
- 587 (46) Narainsamy, K.; Farci, S.; Braun, E.; Junot, C.; Cassier-Chauvat, C.; Chauvat, F. Oxidative-
588 Stress Detoxification and Signalling in Cyanobacteria: The Crucial Glutathione Synthesis
589 Pathway Supports the Production of Ergothioneine and Ophthalmate: Ophthalmate an
590 Evolutionary-Conserved Stress Marker. *Molecular Microbiology* **2016**, *100* (1), 15–24.
591 <https://doi.org/10.1111/mmi.13296>.
- 592 (47) Narainsamy, K.; Marteyn, B.; Sakr, S.; Cassier-Chauvat, C.; Chauvat, F. Genomics of the
593 Pleiotropic Glutathione System in Cyanobacteria. In *Advances in Botanical Research*;

- 594 Elsevier, 2013; Vol. 65, pp 157–188. [https://doi.org/10.1016/B978-0-12-394313-2.00005-](https://doi.org/10.1016/B978-0-12-394313-2.00005-6)
595 6.
- 596 (48) Bellini, E.; Varotto, C.; Borsò, M.; Rugnini, L.; Bruno, L.; Sanità di Toppi, L. Eukaryotic
597 and Prokaryotic Phytochelatin Synthases Differ Less in Functional Terms Than Previously
598 Thought: A Comparative Analysis of *Marchantia Polymorpha* and *Geitlerinema* Sp. PCC
599 7407. *Plants* **2020**, *9* (7), 914. <https://doi.org/10.3390/plants9070914>.
- 600 (49) Kelly, D. J. A.; Budd, K.; Lefebvre, D. D. The Biotransformation of Mercury in PH-Stat
601 Cultures of Microfungi. *Canadian Journal of Botany* **2006**, *84* (2), 254–260.
602 <https://doi.org/10.1139/b05-156>.
- 603 (50) Jones, G. J.; Palenik, B. P.; Morel, F. M. M. TRACE METAL REDUCTION BY
604 PHYTOPLANKTON: THE ROLE OF PLASMALEMMA REDOX ENZYMES. *J Phycol*
605 **1987**, *23* (s2), 237–244. <https://doi.org/10.1111/j.1529-8817.1987.tb04131.x>.
- 606 (51) Schaefer, J. K.; Morel, F. M. M. High Methylation Rates of Mercury Bound to Cysteine by
607 *Geobacter Sulfurreducens*. *Nature Geoscience* **2009**, *2* (2), 123–126.
608 <https://doi.org/10.1038/ngeo412>.
- 609 (52) Schaefer, J. K.; Rocks, S. S.; Zheng, W.; Liang, L.; Gu, B.; Morel, F. M. M. Active
610 Transport, Substrate Specificity, and Methylation of Hg(II) in Anaerobic Bacteria.
611 *Proceedings of the National Academy of Sciences of the United States of America* **2011**, *108*
612 (21), 8714–8719. <https://doi.org/10.1073/pnas.1105781108>.
- 613 (53) Du, W.; Liu, Y.; Sun, J.; Wu, N.; Mai, Y.; Wang, C. The Aquatic Microbial Community: A
614 Bibliometric Analysis of Global Research Trends (1991–2018). *fal* **2020**, *194* (1), 19–32.
615 <https://doi.org/10.1127/fal/2020/1305>.
- 616 (54) Basińska, A. M.; Reczuga, M. K.; Gąbka, M.; Stróżecki, M.; Łuców, D.; Samson, M.;
617 Urbaniak, M.; Leśny, J.; Chojnicki, B. H.; Gilbert, D.; Sobczyński, T.; Olejnik, J.;
618 Silvennoinen, H.; Juszczak, R.; Lamentowicz, M. Experimental Warming and Precipitation
619 Reduction Affect the Biomass of Microbial Communities in a Sphagnum Peatland.
620 *Ecological Indicators* **2020**, *112*, 106059. <https://doi.org/10.1016/j.ecolind.2019.106059>.
- 621 (55) Lürling, M.; Eshetu, F.; Faassen, E. J.; Kosten, S.; Huszar, V. L. M. Comparison of
622 Cyanobacterial and Green Algal Growth Rates at Different Temperatures: *Temperature and*
623 *Phytoplankton Growth Rates*. *Freshwater Biology* **2013**, *58* (3), 552–559.
624 <https://doi.org/10.1111/j.1365-2427.2012.02866.x>.
- 625 (56) Ji, M.; Liu, Z.; Sun, K.; Li, Z.; Fan, X.; Li, Q. Bacteriophages in Water Pollution Control:
626 Advantages and Limitations. *Front. Environ. Sci. Eng.* **2021**, *15* (5), 84.
627 <https://doi.org/10.1007/s11783-020-1378-y>.
628